

Radar Observations of Insects in Free Flight

Radar tracking of single insects in the atmosphere leads to detection of distinctive phenomena.

Kenneth M. Glover, Kenneth R. Hardy, Thomas G. Konrad,
W. N. Sullivan, A. S. Michaels

There has long been disagreement over the nature of many of the so-called "angel" echoes which are commonly observed by radar from regions of apparently clear atmosphere (1). Birds, insects, and atmospheric refractivity perturbations are usually mentioned as sources of these echoes; however, the relative importance of one source in a given series of measurements is clouded by the almost total lack of quantitative measurements of radar backscatter for either known insect flights or refractivity perturbations. The object of the experiments discussed here was to extend our basic knowledge of the radar backscattering properties of insects in free flight and knowledge of the characteristics of these flights, in order to distinguish echoes from insects from those due to clear air phenomena.

A number of cooperative experiments were performed during the summer of 1965 by the Air Force Cambridge Research Laboratories, the Applied Physics Laboratory of Johns Hopkins University, and the Entomology Research Division of the U.S. Department

of Agriculture. This article presents the results of these quantitative observations of single insects in free flight, made with the ultrasensitive radars of the Joint Air Force-NASA (JAFNA) multiwavelength radar facility at Wallops Island, Virginia.

First, let us briefly consider the available theory of radar backscattering from small but complex targets such as insects.

The power, P_r , received by a radar from a point target located at a distance r from the radar is given in standard texts on radar (2) as

$$P_r = \frac{P_t G^2 \lambda^3}{(4\pi)^3 r^4} \sigma$$

where P_t is the transmitted power, G is the one-way antenna gain, λ is the radar wavelength, and σ is the radar backscatter cross section of the target. Of the various terms in the radar equation, only σ is a characteristic of the target; it is a measure of the target's efficiency for scattering radiation back to its source and may be defined as [(power reflected toward source per unit solid angle) / (incident power density / 4π)] or, alternatively, as

$$\sigma = \lim_{r \rightarrow \infty} 4\pi r^2 \left| \frac{E_r}{E_i} \right|^2$$

where E_r and E_i are the strengths of the reflected and incident electric fields, respectively.

In principle, the strength of the reflected field, and hence σ , is found by solving Maxwell's equations subject to the appropriate boundary conditions; however, in actual practice, rigorous solutions have been found for only the simplest of shapes (2). The usual approach is to make up to fourth-order approximations in order to arrive at a theoretical value of σ . Such computations are valid for a certain polarization and frequency range of incident radiation and a target of specific shape and dielectric constant.

Predicting the radar cross section of a given insect on the basis of existing theory is a difficult task, for the microwave dielectric constant for various species of insects is unknown and the body is usually not a well-defined geometric shape such as a sphere, a prolate spheroid, or an ogive. In the discussion which follows, we therefore do not pursue the theoretical problem but, instead, proceed to some of the distinguishing features of experimental tracks of individual insects in free flight.

Observations

Three high-powered, high-sensitivity radars of differing wavelengths were used in these experiments. The characteristics of the three radars are shown in Table 1. The radar of 10.7-centimeter wavelength, with an automatic tracking capability, was used as the primary source of position data; the 3.2- and 71.5-centimeter systems shared an antenna which was slaved, in azimuth and elevation, to the antenna of the 10.7-centimeter system to permit simultaneous multiwavelength measurements of radar cross sections.

Insect specimens were fed sugar water, placed in individual containers, and then loaded aboard a small single-engine aircraft. Once airborne, the aircraft was picked up by the automatic tracking system of the 10.7-centimeter radar, and the aircraft was then vectored along a radar radius parallel to the vector of the prevailing wind. The plane continued on an outbound

Table 1. Characteristics of three radars of the Joint Air Force-NASA (JAFNA) radar facility.

Wave-length (cm)	Antenna diameter (m)	Antenna beam-width (deg)	Pulse length (10^{-6} sec)	Antenna gain (db re isotropic radiator)	Minimum detectable signal (dbm)	Peak transmitted power (10^6 watts)	Minimum detectable cross section at 10 km (cm^2)	Diameter of water sphere of equivalent cross section (cm)
3.2	10.4	0.21	2.0	58	-101	0.9	1.82×10^{-2}	0.43
10.7	18.4	.48	2.0	51	-110	3.0	1.55×10^{-5}	.30
71.5	18.4	2.9	2.0	35	-105	6.0	1.62×10^{-4}	1.57

Table 2. Physical characteristics of the test insects.

Species and sex	Wing-spread (cm)	Body length (cm)	Fresh weight (g)	Water content (%)
<i>Manduca sexta</i> (hawkmoth), male	10	5.0	1.0-1.5	64.1
<i>Heliothis virescens</i> (tobacco budworm moth), male and female	3.0	1.9	0.14	60
<i>Apis mellifera</i> (honeybee), worker	1.0	1.5	0.08-0.11	66.3

radial course until the altitude and the distance from the radar were at least 1.5 and 10 kilometers, respectively. If the region surrounding the aircraft was then observed to be completely free of all other radar targets, a single insect specimen was ejected into the slipstream of the aircraft. Simultaneously, the automatic tracking of the aircraft was halted, with the radar beam fixed upon the drop zone. As the plane continued moving away from the radar it gradually passed out of the primary radar beam, leaving just

the sample insect in free flight within the drop zone.

In 9 to 10 seconds after release of the insect this separation of targets appeared on the radar as an insect echo of relatively small amplitude, gradually breaking away from the much stronger aircraft echo. Approximately 30 seconds after release the two echoes were separated sufficiently in range for the automatic tracking circuitry of the 10.7-centimeter radar to follow only the insect. Once a specimen was picked up by the automatic

system, signals proportional to the power received from the targets were recorded by means of an X-Y plotter, with time as the abscissa. Azimuth, elevation, and range data were sampled simultaneously once every second and recorded on a high-speed printer.

In all, four different species of insects were studied at altitudes from 1.6 to 3.0 kilometers and temperatures from 7° to 13°C. Three of these species—hawkmoths (adult form of a tobacco hornworm), tobacco budworm moths, and honeybees—were reared at the Tobacco Insects and Apiculture Laboratories of the Entomology Research Division, U.S. Department of Agriculture. Data on the water content and other pertinent physical characteristics of the test insects are given in Table 2 (3). Corresponding data for the fourth species studied, native dragonflies, were not available.

A typical 2-minute sample of radar observations of the track of a hawkmoth is shown in Fig. 1. Except for brief climbs at the beginning and end of the track (Fig. 1a), the insect's altitude decreased at a nearly constant rate of about 6.3 meters per second. In Fig. 1b the ground position for 10-second intervals over the 2-minute period is shown, together with a vector corresponding to a 2-minute average of the wind velocity encountered by the insect. A comparison of the average velocities for insect and wind shows that the insect must have been moving with an average air velocity of 1.3 meters per second at an angle of 128 degrees relative to the mean wind direction. This insect velocity is slightly larger than would be expected on the basis of errors in measurement of the winds. Thus, it appears that the hawkmoth was flying during at least some parts of the track shown in Fig. 1.

A continuous 2-minute record of the radar cross section, σ , of the hawkmoth, as measured with the 10.7-centimeter radar, is shown in Fig. 1c, and a shorter but expanded (in time) version of the same record is shown in Fig. 1d. Note the time periods in which σ varies relatively slowly over a two-orders-of-magnitude interval, and similar periods of relative calm in which σ fluctuates at a high frequency and the values for σ deviate from the mean of 1 square centimeter by a factor of less than 2. The mean magnitude and the fluctuations of σ are due to a combination

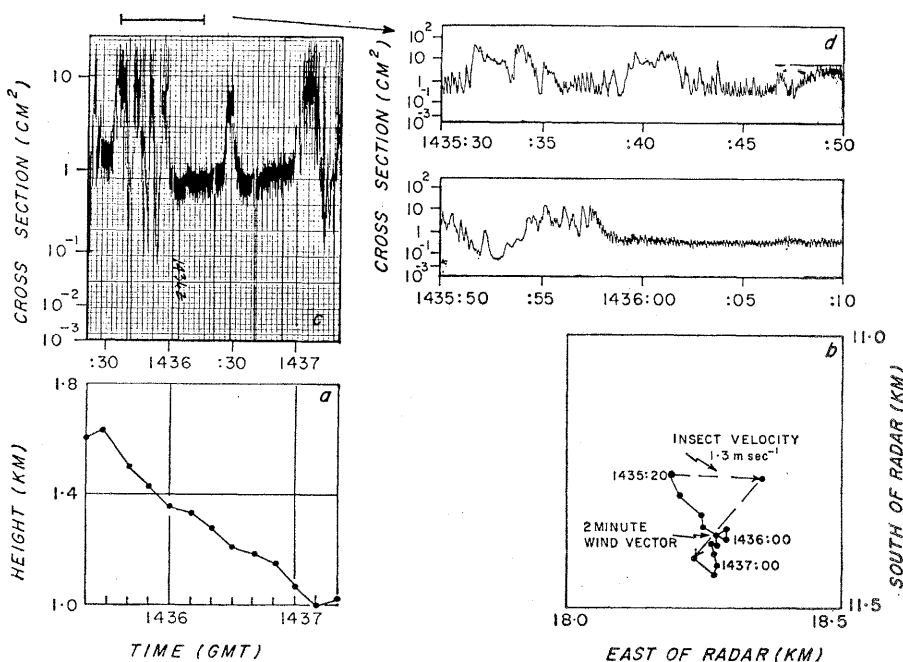


Fig. 1. Tracking data for a winged hawkmoth (see text). Note the periods of large-amplitude changes in the cross section, and similar periods where the fluctuations are of lower amplitude but higher frequency. In (d) the scale for the abscissa is in hours, minutes, and seconds.

of factors: (i) insect size and shape, (ii) moisture content of the wings, (iii) orientation of the insect body relative to polarization of the incident radiation, and (iv) wing motion. Factors (i) and (ii) affect the magnitude of the variations in cross section and are constant for a given insect. But changes in the orientation of either the insect's body or its moisture-filled wings relative to the polarization of the incident radiation result in fluctuations in σ . Unless the changes in orientation of body and of wings occur with the same frequency and produce the same magnitude of change in σ , the two effects should generally be resolvable. Certainly the traces of Fig. 1 suggest that two distinct phenomena are taking place. There is no correlation between the large-amplitude variations in σ and the changes in path (hence long-term orientation) indicated by the position data obtained in the second-by-second sampling. Moreover, the alternating presence and absence of the amplitude fluctuations suggest that the large fluctuations may be occurring when the moth is flying and that the relatively calm periods may correspond to intervals of gyration, tumbling, or other nonflying body motion.

As a partial check upon the validity of the foregoing hypothesis, the wings of another hawkmoth were clipped near the body and the wingless moth was then released from the aircraft. The corresponding radar observations are shown in Fig. 2. In this case the insect has a slightly greater downward velocity of 8.0 meters per second and an average air velocity of 1 meter per second, directed along the wind. This air velocity gives a measure of the uncertainty in the wind measurements. The track of this moth confirms the supposition that the winged hawkmoth was flying during part of its track.

The cross-section data for the wingless hawkmoth are shown in Fig. 2, c and d. The average magnitude of the cross section for this wingless moth is smaller than that for the winged one; however, this result was to be expected, for this specimen was slightly smaller than the moth of Fig. 1, and the wing-clipping procedure removed at least a few drops of body fluid.

The most notable feature of Fig. 2, c and d, is the absence of the large-amplitude, low-frequency component

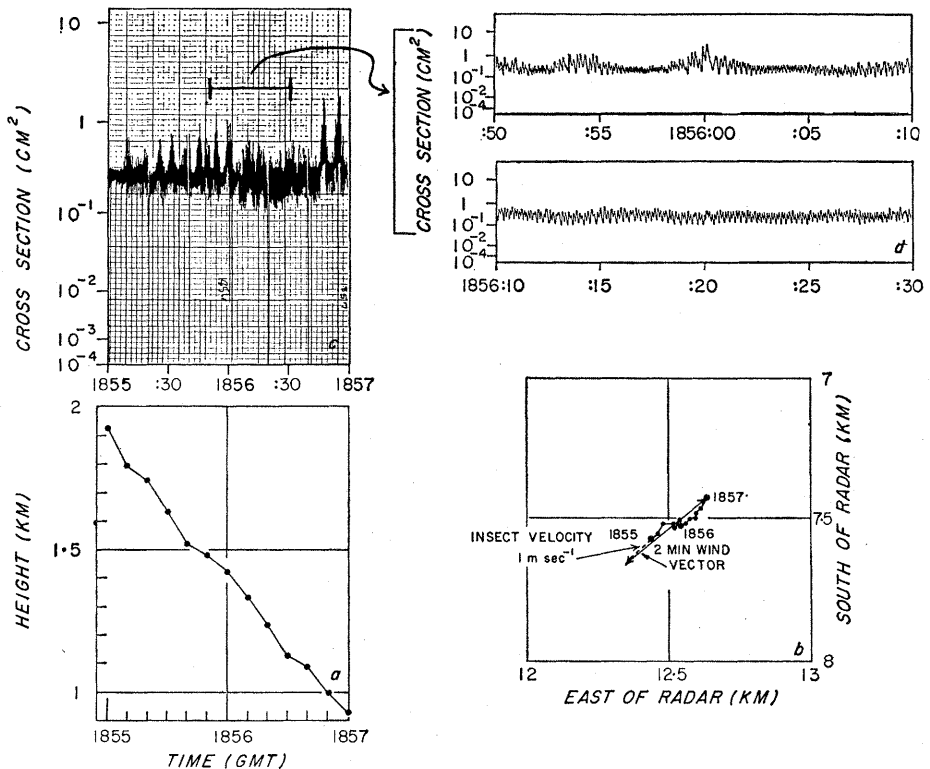


Fig. 2. Tracking data for a wingless hawkmoth. Note both the absence of the large-amplitude fluctuations observed for the winged specimen and the presence of bursts of small oscillations in the cross section, not observed for the winged specimen.

of the fluctuations in σ . Again, this strongly suggests that the winged moth must have been slowly moving its wings during the periods when the large fluctuations were observed. Similarly, the periods of relatively low-amplitude, high-frequency fluctuations of Fig. 1 must have been associated with some form of oscillatory body motion.

The cross-section traces of Fig. 2 are marked by bursts of up to 3-second duration in which fluctuations in σ increase by as much as a factor of 4 over what appears to be a steady value for background fluctuations. Without visual observations of actual body motion, it is difficult to verify the origin of these fluctuations. Changes in the orientation of the insect relative to polarization of the incident radiation were noted throughout the test period; however, it is not possible to explain the observed fluctuations on the basis of these orientation changes alone. In subsequent laboratory observations of winged and wingless hawkmoths anesthetized with carbon dioxide and dropped in quiet air from a height of 6 meters, the winged moths gyrated to the ground with the head angled downward and the wings fixed tangential to the helical gyration path. The wing-

less specimens, because of their lack of wing stabilization, generally exhibited a more erratic gyration or wobbling motion. If the nonflying body motion of the winged moth of Fig. 1 was similar to the falling motion of the winged anesthetized laboratory moths, the winged hawkmoth must have steadily gyrated downward, presenting an oscillating orientation relative to the polarization of incident radiation during the periods when the low-amplitude, high-frequency fluctuations in σ were observed. Similarly, the steady background fluctuation of σ in Fig. 2 probably corresponds to the gyrating component of the wingless specimen's erratic motion, and the bursts in the cross-section record probably correlate with the periods in the wobbling motion when the major axis of the hawkmoth's body was most nearly aligned with the polarization.

The tracking data for the smaller moth, the tobacco budworm moth, are shown in Fig. 3. This species had a smaller downward velocity (3.8 meters per second) and a greater average air velocity (2.4 meters per second at an angle of 147 degrees to the mean wind) than the hawkmoths had. The cross-section data for the tobacco budworm moth presented in Fig. 3, c and

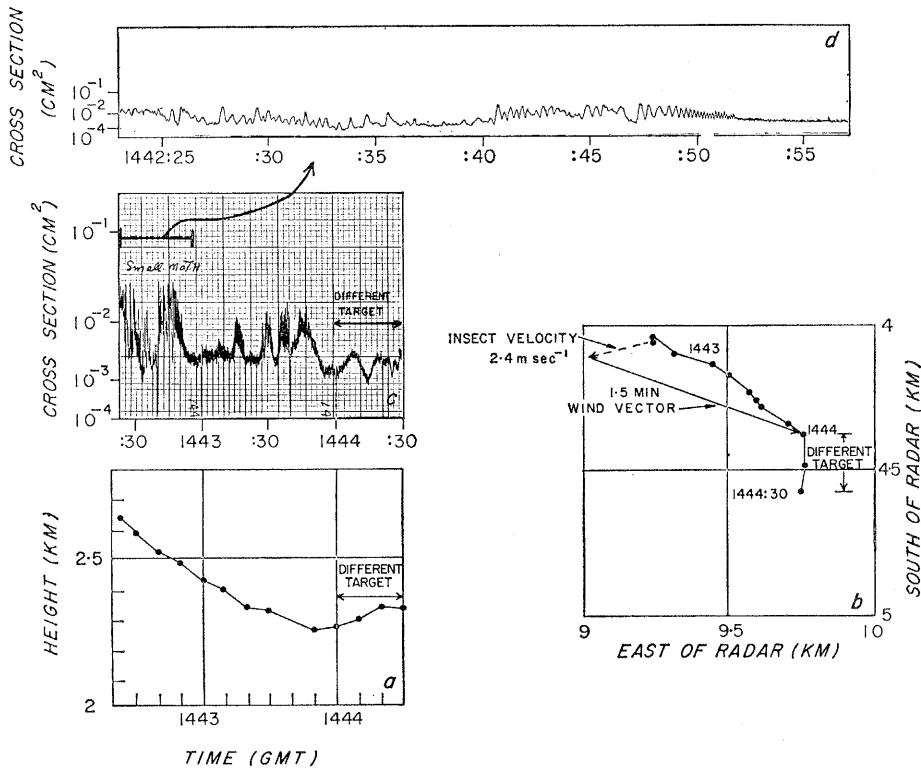


Fig. 3. Tracking data for the tobacco budworm moth. Note the large-amplitude, high-frequency oscillations at the beginning of the cross-section record (d), followed by alternating periods of relative calm and shorter periods of high-amplitude, high-frequency oscillation.

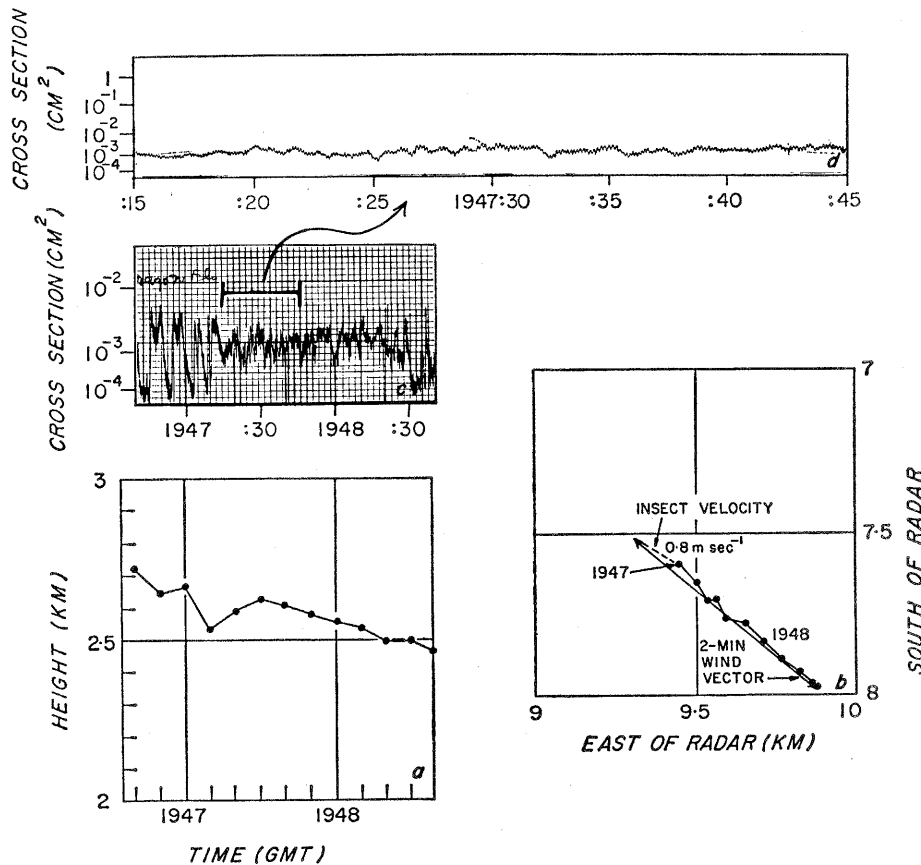


Fig. 4. Tracking data for the dragonfly. Note the large-amplitude, low-frequency (approximately $\frac{1}{2}$ cycle per second) fluctuations at the beginning of (c), the 2-minute cross-section record. The frequency of the very-low-amplitude modulation shown in trace (d) begins at 9.0 cycles per second at left and decreases to 7.2 cycles per second at right.

d, show a marked decrease in magnitude, with the value for background fluctuation falling to a mean of about 2×10^{-3} square centimeter. Once again there are relatively large fluctuations in σ , especially between 14h 42' 23" and 14h 42' 52" (Fig. 3d). If the analysis given above of the hawkmoth tracks is correct, then the tobacco budworm moth was probably flying during this interval and also during two shorter periods, 14h 43' 27" to 14h 43' 33" and 14h 43' 35" to 14h 43' 40". Similarly, the peaks in the cross section at 14h 43' 16" and 14h 43' 47" are believed to be due to changes in body orientation rather than to flying, because of the lack of any large-amplitude, high-frequency oscillations in σ .

The next insect studied was a small dragonfly approximately 3 centimeters long. This insect, unlike the moths, has thin filmy wings which are nearly moisture-free and a long slender body which is very nearly a prolate spheroid of small eccentricity (< 0.2). The tracking data for this insect are shown in Fig. 4. The average downward velocity of 1.9 meters per second is smaller, and the average air velocity of 0.8 meter per second is at a greater angle relative to the mean wind direction, than the averages for either of the moths.

The cross-section records of Fig. 4 also show large-amplitude fluctuations, especially near the beginning of the 2-minute record; however, the periods of these fluctuations are much greater than the periods observed for either of the moths. In the absence of visual observations it is again difficult to be certain of the origin of these fluctuations. They could hardly be due to wing flapping, for dragonfly wings lack a sufficient concentration of moisture to influence σ to the extent observed in Fig. 4. It is possible that either the major axis of the insect body was slowly gyrating relative to the polarization of incoming radiation or the body was tumbling end over end. Either event could explain the data, in terms of both the magnitude and the frequency of the fluctuations. In the portion of the track that follows these large fluctuations the cross-section record stabilizes to a mean value of 1.2×10^{-3} square centimeter and there is a noticeable lack of high-amplitude, high-frequency fluctuations in the expanded trace (Fig. 4d). The small-amplitude oscillations which occur throughout Fig.

4d steadily decrease in frequency from an average of 9.0 cycles per second during the first 5-second interval to an average of 7.2 cycles per second over the last interval. These frequencies are in reasonably good accord with the dragonfly wing-beat frequencies expected at these temperatures (7° to 10°C). Wing-beat frequencies of 41 to 46 beats per second at room temperature are reported (4) for the dragonfly; however, this beat frequency decreases rapidly with reduction in temperature. It is found, for example, that there is a 23-percent decrease in the wing-beat frequency of the sheep blowfly (*Phaenicia sericata*) when the ambient temperature is reduced by only 10° at 30°C (5). A frequency of 9 cycles per second is therefore a realistic value for the dragonfly at 7° to 10°C . If these very-small-amplitude fluctuations are associated with wing flapping, then either the wings must make a sufficient contribution to the total cross section to be detectable or the body recoil following wing beats must sufficiently alter the body orientation to produce a modulation in the amplitude of σ .

The results for the fourth species studied, the worker honeybee, are shown in Fig. 5. The uncertainty indicated by the word *probably* in the figure legend arose from the fact that pickup of the track by the automatic tracking system took 12 seconds longer than the fairly standard time of 30 seconds observed for the other insects; however, the "probable" honeybee was first observed after 9 seconds, as in the case of the other insects, and the same (or what appeared to be the same) object remained in view until picked up by the automatic system. Thus, there is a fairly high probability that the object tracked was actually a honeybee, but there is also a small possibility that another object moved into the beam during the relatively long period before pickup and was subsequently tracked.

The honeybee track is marked by a nearly horizontal path, a high average air velocity (6.7 meters per second at an angle of 72° to the mean wind), and a relatively constant cross section (mean, 3.6×10^{-3} square centimeter). Intuitively, one expects a more constant cross section on the basis of the earlier observations, for the wings of the honeybee are filmy and probably never make a significant contribution to σ . Moreover, the body

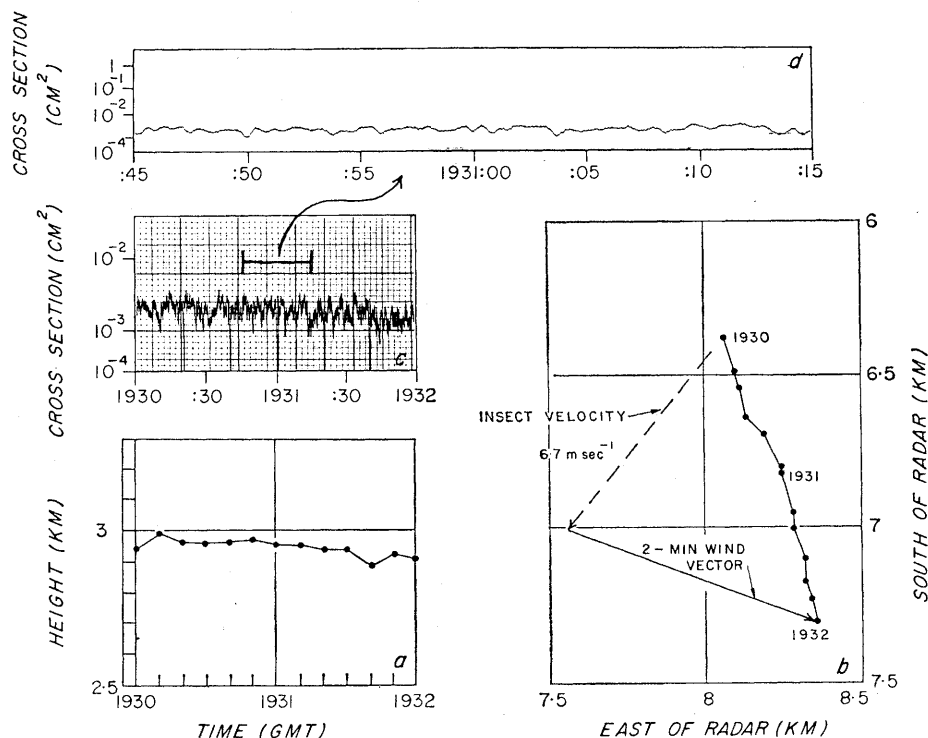


Fig. 5. Tracking data for, probably, one honeybee (see text). Note the relatively large air velocity of the honeybee and the absence of any large-amplitude, high-frequency fluctuations in the cross sections.

of the honeybee is more nearly spherical than that of any of the other insects studied, hence the cross sections are less dependent upon the aspect angle.

It is important to note that the manner in which σ varies in each of the expanded time records of Figs. 1d, 3d, 4d, and 5d is distinctly different for each of the species. This is due in part to the fact that each species is distinctly different from the others in overall size, natural wing-beat frequency, wing moisture content, and other physical properties. And it is also due in part to differences in the response of each species to a sudden change of environment. Spectral analysis of these records would accordingly show distinct differences in the fluctuation spectra for different species, and in the fluctuation spectra for the same insect over a period of time. It is quite difficult to draw meaningful comparisons of these spectra without supportive visual observations from which to identify comparable origins of the fluctuations. But certainly the correlation of the spectral characteristics with the physical parameters of insect flight and the comparison of these characteristics for various species give promise of providing the entomologist with a powerful tool.

Previous experience has shown that,

at the radar ranges used in these experiments, errors associated with the direction of the narrow radar beams to the same point in space during tracking are sufficiently large, even with partial (azimuth only) electronic parallax correction, that representative long-term measurements of cross sections are obtainable only with the 10.7-centimeter automatic tracking radar. In order to make sure that the beams of the 3.2- and 71.5-centimeter radars were boresighted on the same target as the beams of the 10.7-centimeter system for at least part of the time during a track, the antenna of the 3.2- and 71.5-centimeter radars was periodically "unslaved" in elevation from the automatic system and an operator manually positioned the antenna until the signal amplitude peaked. The antenna was then "unslaved" in azimuth, and the process was repeated. Usually only slight adjustments in azimuth and elevation were required to obtain the peak signal with the 3.2-centimeter system. The maximum cross sections observed by this means at 3.2-centimeter wavelength for the wingless hawkmoth, the dragonfly, and the probable honeybee of Fig. 5 are shown in Fig. 6, together with observations obtained simultaneously at 10.7 centimeters. These 10.7-centimeter data

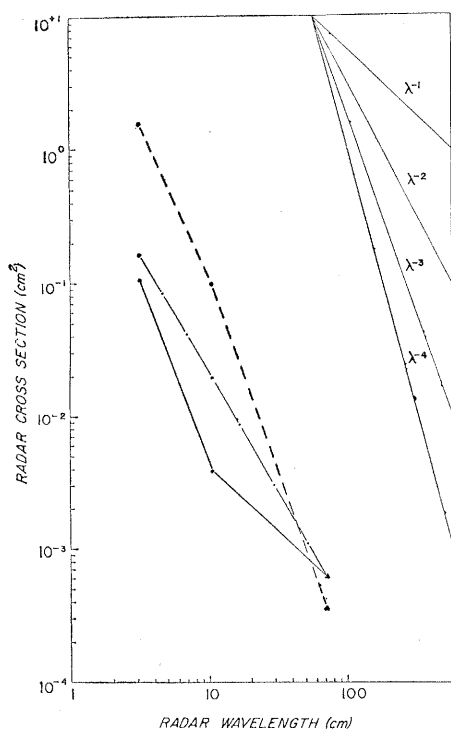


Fig. 6. Radar cross sections of insects as a function of the radar wavelength, for a wingless hawkmoth (dashed curve), a honeybee (dot-dashed curve), and a dragonfly (solid curve). See text for interpretation of the points at 71.5-centimeter wavelength. The data represent coincident observations at each wavelength. For reference, lines of slope corresponding to an indicated wavelength dependence are shown at upper right.

were obtained on the basis of coincidence with the 3.2-centimeter observations, hence they differ slightly from the mean values reported above. The absolute cross sections shown in Fig. 6 are typical of those observed. Moreover, the cross section for the honeybee (0.2 square centimeter) is in good agreement with values, recently obtained with a 3.2-centimeter wavelength backscatter facility, of 1.0 and 0.3 square centimeter when the polarization of the incoming radiation is aligned with the longitudinal and transverse axes, respectively (6). At both 3.2- and 10.7-centimeter wavelengths the absolute cross sections for the three specimens of Fig. 6 are seen to vary in a complex manner with body length, for the cross section of the honeybee is intermediate between cross sections of the hawkmoth and the dragonfly, yet both the hawkmoth and the dragonfly are much longer than the honeybee. A similar effect was noted in the measurements made with a backscatter facility (6).

As is usually observed with targets whose body dimensions are of the order of 0.1λ or greater, the insects of Fig. 6 do not exhibit a simple power-law relationship between cross section and radar wavelength. At wavelengths between 3.2 and 10.7 centimeters the cross sections depended on wavelength between the limits of $\lambda^{-2.7}$ and $\lambda^{-1.8}$. The 71.5-centimeter radar system failed to detect even the largest of the specimens, and thus the actual cross sections of the insects at the longer wavelength fall somewhere below the minimum detectable cross sections denoted in Fig. 6 by points at 71.5 centimeters. At wavelengths between 10.7 and 71.5 centimeters the curves therefore place an upper bound on the wavelength dependence at λ^{-3} .

Discussion

These observations have implications for both radar meteorology and entomology. In the area of meteorology, Hardy and his associates (7) have concluded from previous studies that the mysterious discrete "dot angel" echoes observed from invisible targets in the apparently clear atmosphere are, in large measure, due to insects. These conclusions are based upon extensive multiwavelength observations of the "dot angel" echoes, obtained with the same radars as those used in our studies and with techniques similar to ours.

It has been found, for example, that the "dot angel" echoes appear to be highly localized point targets; the targets, at a given time and point in space, have nearly equal cross sections; the targets can be tracked for as long as 35 minutes; they frequently have a significant velocity relative to the mean wind velocity, and they are not observed in winter. Moreover, no single coherent atmospheric surface could be found to explain the combination of cross-section observations, at a wavelength of 3.2 centimeters, in the range of 0.05 to 0.5 square centimeter; a cross-section wavelength dependence of λ^{-1} to λ^{-2} at wavelengths between 3.2 and 10.7 centimeters; and a wavelength dependence of approximately λ^{-4} at wavelengths between 10.7 and 71.5 centimeters.

The observations presented here confirm the view that insects are highly

localized point targets which can be tracked for long periods and which may or may not have a significant velocity at a large angle to the wind direction. Moreover, the cross sections are seen to be in the range from 0.1 to 1.6 square centimeters at wavelength of 3.2 centimeters, and to vary as $\lambda^{-2.7}$ and $\lambda^{-1.8}$ at wavelengths between 3.2 and 10.7 centimeters and as something less than λ^{-3} at wavelengths between 10.7 and 71.5 centimeters. The correlation between present and past (7) observations is quite good as to both absolute magnitude and wavelength dependence of the cross sections. The data thus strongly suggest that "dot angel" echoes having characteristics similar to those described above are in fact due to insects.

In the area of entomology, the utility of these experiments lies not with a particular observation but rather in the demonstration that radar can be successfully used to measure entomologically significant parameters which have heretofore been considered largely unmeasurable. For example, it appears from these studies that radar is of value to the entomologist in tracking insect flight and insect behavior patterns and migration; in determining free-flight azimuth, elevation, range, and velocity of single insects; and in making studies to determine the uniqueness of cross-section fluctuation spectra for a given species. Indeed, there is every reason to believe that the entomologist, like the meteorologist, will soon be using radar as a tool.

References and Notes

1. A. W. Friend, *Proc. I.R.E. (Inst. Radio Engrs.)* **37**, 116 (1949); A. B. Crawford, *ibid.*, p. 404; V. G. Plank, "A meteorological study of radar angels," *Air Force Cambridge Res. Lab. Geophys. Res. Paper No. 52* (1956), p. 117; D. Atlas, *Advan. Geophys.* **10**, 317 (1964).
2. For example, D. E. Kerr, *Propagation of Short Radio Waves* (McGraw-Hill, New York, 1951), p. 445.
3. P. A. Giang and M. S. Schechter, in preparation.
4. C. H. Greenwalt, *Smithsonian Inst. Misc. Collections* **144**, 16 (1962).
5. W. J. Yurkiewicz and T. Smyth, Jr., *J. Insect Physiol.* **12**, 189 (1966).
6. R. G. Hajovsky, A. P. Deam, A. H. La Grone, *IEEE (Inst. Elec. Electron. Engrs.) Trans. Antennas Propagation* **14**, 224 (1966).
7. K. R. Hardy, D. Atlas, K. M. Glover, *J. Geophys. Res.* **71**, 1537 (1966).
8. This research has been supported by the AFRL Laboratory Director's Fund and NASA Wallops Station. We thank Dr. D. Atlas, Mr. I. Katz, and Dr. E. F. Knipling for their encouragement and suggestions, Dr. S. Vogel, Dr. K. A. Browning, Mr. S. A. Hall, and Mr. R. J. Donaldson for valuable discussions, and Mr. C. R. Landry, Mr. J. Howard, Mr. R. Masek, and the staff of the JAFNA radar facility, Wallops Island, Virginia, for their cooperation.